Aerosol and Air Quality Research, 17: 1798–1808, 2017

ISSN: 1680-8584 print / 2071-1409 online
doi: 10.4209/aaqr.2017.05.0188

Novel Method for Preparing Controllable Nanoporous α-Fe_2O_3 and its Reactivity to SCR De-NO_x

Haibo Liu[1], Zexin Zhang[1], Qian Li[1], Tianhu Chen[1*], Changai Zhang[1], Dong Chen[1], Chengzhu Zhu[1], Yang Jiang[2]

[1] *Laboratory for Nanomineralogy and Environmental Material, School of Resources & Environmental Engineering, Hefei University of Technology, Hefei, Anhui 230009, China*
[2] *School of Materials Science and Engineering, Hefei University of Technology, Hefei, Anhui 230009, China*

ABSTRACT

Controllable nanoporous hematite (CNH, α-Fe_2O_3) was prepared by thermal treatment of α-FeOOH at different temperatures, and the SCR activity of the prepared α-Fe_2O_3 was evaluated. XRD (X-ray diffraction), HRTEM (high-resolution transmission electron microscopy), N_2 adsorption-desorption, XPS (X-ray photoelectron spectroscopy), and NH_3-TPD (NH_3-temperature programmed desorption) were utilized to characterize the catalysts. The results indicated that after thermal treatment at less than 600°C, the α-Fe_2O_3 catalysts exhibited excellent NO conversion that was higher than 80% in a temperature range from 300 to 400°C. CNH400 with a relatively large surface area of 47.24 m^2 g^{-1} and many surface hydroxyl groups did not exhibit a substantially improved SCR activity even though it exhibited the best SCR activity. Therefore, the L-H mechanism was not the main reaction route for SCR of NO by α-Fe_2O_3. The increasing crystallization of α-Fe_2O_3 decreased the SCR activity, indicating that a decrease in surface oxygen defects was important for the SCR of NO and fitting the E-R mechanism. The NH_3-TPD and XPS (O1s) results confirmed this hypothesis. This study provides an approach for the design and preparation of a controllable nanoporous α-Fe_2O_3 catalyst for SCR of NO by NH_3.

Keywords: α-FeOOH; Controllable nanoporous α-Fe_2O_3; Selective catalytic reduction; Mechanism.

INTRODUCTION

NO_x can be released through natural emissions, such as lightning and microbiological processes, and from anthropogenic sources, such as fossil fuel and biomass burning (Khokhar *et al.*, 2015; Sahu, 2015; Kiros *et al.*, 2017). Selective catalytic reduction (SCR) is an effective method for the reduction of NO_x by NH_3 over various catalysts due to its high efficiency and economic efficiency (Balle *et al.*, 2009; Grossale *et al.*, 2009; Boroń *et al.*, 2015). Among these catalysts, V_2O_5/TiO_2 in combination with MoO_3 and WO_3 has been commercialized due to its high catalytic reactivity. However, some challenges associated with this catalyst, such as a high reaction temperature, narrow operating temperature, the phase transformation of carrier, and environmental toxicity of vanadium species, have attracted attention (Balle *et al.*, 2009; Liu and He, 2010; Liu *et al.*, 2011b; Ma *et al.*, 2011). Therefore, to overcome these challenges, numerous vanadium-free catalysts have been studied, including noble-metal catalysts (Zahaf, 2015), M-zeolite catalysts (M-Fe, Cu, Mn, Mo) (Perezramirez, 2004; Yoshida, 2004; Liu *et al.*, 2011a; Ochońska *et al.*, 2012; Schuricht and Reschetilowski, 2012; Mejri *et al.*, 2016) and metal oxide catalysts (Fe-based oxide catalysts, Mn-based oxide catalysts, Cu-based oxide catalysts, Ce-based oxide catalysts, Cr-based oxide catalysts, etc.) (Kato *et al.*, 1981; Yang *et al.*, 1992; Duffy *et al.*, 1994; Kapteijn *et al.*, 1994; Chen *et al.*, 1995; Schneider *et al.*, 1995; Zhu *et al.*, 2000; Eigenmann *et al.*, 2006; Kang *et al.*, 2007; Xu *et al.*, 2008; Liu *et al.*, 2010; Liu *et al.*, 2013a; Chiu, 2015; Yu, 2015; Yu *et al.*, 2017). Fe-based and Mn-based catalysts have been the most favorable catalysts among the various vanadium-free catalysts. Based on the relatively low amount of Mn in the Earth, Fe-based catalysts are more feasible and economical for industrial application.

The SCR activities of different Fe-based oxide catalysts (i.e., iron oxide and Fe-based catalysts) have been reported, and different reaction mechanisms have been discussed. The reported iron oxide catalysts primarily contained α-Fe_2O_3 (Liu *et al.*, 2013a), γ-Fe_2O_3 (Huang *et al.*, 2013; Yang *et al.*, 2013), rod-shaped Fe_2O_3 (Mou *et al.*, 2012) and Fe-based catalyst including Fe-ZSM-5 (Brandenberger *et al.*, 2010), Fe/HBEA (Ma *et al.*, 2012), Fe-Ti-V spinel (Yang *et al.*, 2012), Fe-Ti spinel (Yang *et al.*, 2016), and Fe-Mn oxides

* Corresponding author.
Tel.: +86 13956099615; +86 0551-62903990
E-mail address: chentianhu@hfut.edu.cn

(Chen *et al.*, 2014). The results indicated that the Fe-based oxide catalyst exhibit excellent SCR performance in a temperature range of 200–400°C. Mou *et al.* (2012) reported that rod-shaped α-Fe_2O_3 could maintain a NO conversion of more than 80% in a temperature range from 200°C to 400°C, and γ-Fe_2O_3 exhibited a better SCR activity than α-Fe_2O_3. In addition, Yang *et al.* (2013) confirmed that both α-Fe_2O_3 and γ-Fe_2O_3 exhibit remarkably different NO conversions. The latter was better due to additional oxygen defects and the formation of few stable nitrates. To improve the stability, operation temperature window and resistance to poisoning, different additives and supports have been employed. The addition of WO_3 can improve the thermal stability and catalytic activity of Fe_2O_3/ZrO_2 (Chen *et al.*, 1995; Apostolescu *et al.*, 2006).

The Langmuir-Hinshelwood (L-H) and Eley-Rideal (E-R) mechanisms have been extensively cited to discuss the reaction route of the SCR of NO. For Fe-based catalysts, the main reaction mechanism is influenced by the type of catalyst and reaction temperature with a focus on the importance of Brönsted and Lewis acid sites. The standard SCR process and rough mechanism are as follows:

Standard SCR: $4NO + 4NH_3 + O_2 \rightarrow 4N_2 + 6H_2O$

L-H mechanism:

$$*^1 - NH_4 + *^2 - NO_2 \rightarrow NO_2(NH_4^+)_2 \xrightarrow{+NO} N_2 + H_2O$$

E-R mechanism: $*^3 - NH_2 + NO \rightarrow N_2 + H_2O$

where the formation of adsorbed NO_2 is the rate-controlling step with respect to the L-H mechanism. $*^{1, 2, 3}$ denoted different adsorption sites. For pure iron oxides, the E–R mechanism, which involves the conversion of NO by reacting amide intermediates and gaseous NO, has been proposed. As previously mentioned, the iron oxide and Fe-based catalyst exhibit good SCR activity, and the reaction mechanism has been discussed in detail. However, nanoporous α-Fe_2O_3 and the effect of the pore texture on the NO conversion has not been previously reported.

α-FeOOH is a type of hydroxyl-rich iron oxyhydroxyl (Liu *et al.*, 2014), which is different from Fe-based catalysts. In addition to these bulky groups, α-FeOOH still has a complicated surface structure, especially the distribution of adsorbed water/hydroxyl groups, which are illustrated in a previous report (Haibo *et al.*, 2013). Therefore, α-FeOOH was chosen as a precursor to prepare nanoporous α-Fe_2O_3 due to its thermal decomposition characteristics at different temperatures. The objective of this study was to prepare controllable nanoporous hematite (CNH, α-Fe_2O_3) by thermal treatment of α-FeOOH and evaluate the SCR activity of different CNH catalysts. The effect of the preparation temperature on the porous texture of the newly formed α-Fe_2O_3 was investigated, and the relationship between the pore texture and the SCR activity is discussed relative to the NO conversion as well as the TEM, N_2 adsorption-desorption, XPS and NH_3-TPD characterization.

EXPERIMENTAL

Catalyst Preparation

The nanoporous α-Fe_2O_3 (CNH) catalysts were prepared by thermal treatment of α-FeOOH in air for 1 h at various temperatures (400, 500, 600, 700, 800°C). Thermal treatment was carried out in a tube furnace with a temperature-programmed controller using 10 °C min^{-1} as the heating rate. The particle size was controlled between 0.25 mm (60 mesh) and 0.38 mm (40 mesh) by sieving. To simplify the sample labels, an abbreviation was used. CNH400 refers to the α-Fe_2O_3 catalyst obtained by thermal treatment of α-FeOOH at 400°C.

Catalyst Activity Testing

The SCR of NO by NH_3 was carried out in a fixed-bed quartz tube reactor with an inner size of 8 mm, and 1 g of catalyst was used each time. The typical reactant gas contained 500 ppm of NO, 500 ppm of NH_3, 3% of O_2, and balanced with Ar, and a gas flow rate of 300 mL min^{-1} was controlled by mass flow controllers (Sevenstar D08, Beijing). The catalytic activity testing was carried out in a temperature range of 150–400°C with a gas hourly space velocity (GHSV) of 72,000 h^{-1}. The temperature was regulated via a temperature-programmed controller. The concentration of NO, NO_2, NH_3, and N_2O were monitored using a Fournier transform IR (FTIR) spectrometer. The schematic diagram of the experimental setup is shown in Fig. 1.

As the SCR reaction reached a steady state, the ratio of NO conversion and N_2 selectivity were calculated using the following equations:

$$\text{NO conversion} = \frac{[NO]_{in} - [NO]_{out}}{[NO]_{in}} \times 100\% \quad (1)$$

$$N_2 \text{ selectivity} = \frac{[NO_x]_{in} + [NH_3]_{in} - [NO_x] - [NH_3] - 2 \times [N_2O]_{out}}{[NH_3]_{in} - [NH_3]_{out} + [NO_x]_{in} - [NO_x]_{out}} \times 100\% \quad (2)$$

$$[NO_x] = [NO] + [NO_2] \quad (3)$$

Catalyst Characterization

X-ray diffraction (XRD) measurements were carried out on a Rigaku D/max diffractometer using Cu Kα radiation (50 kV and 100 mA). The diffraction patterns were recorded between 15° and 70° with a step size of 4 ° min^{-1}.

A high-resolution transmission electron microscope (HRTEM, JEM-2100) was employed to characterize the morphology and pore structure of the catalysts.

The specific surface area, pore volume and pore size distribution were measured by N_2 adsorption-desorption at liquid nitrogen temperature with a Quantachrome NOVA 3000e analyzer. The samples were first degassed at 110°C for 24 h.

The X-ray photoelectron spectroscopy (XPS) data were obtained with an ESCALAB250Xi electron spectrometer

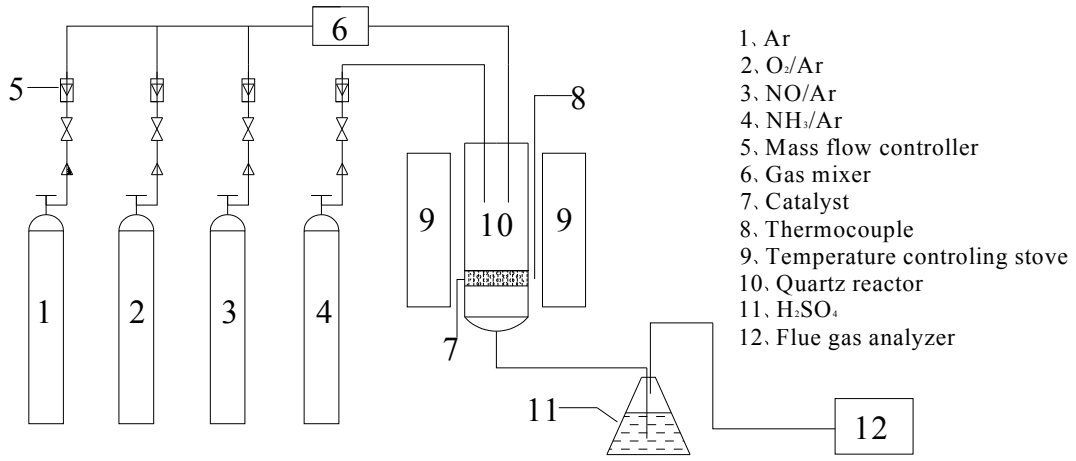

Fig. 1. Schematic diagram of the SCR of NO by NH_3 over different nanoporous α-Fe_2O_3 catalysts.

from Thermo Fisher Scientific using Al Kα radiation. The binding energies were referenced to the C 1s line at 284.7 eV.

Temperature-programmed desorption of NH_3 (NH_3-TPD) was employed to characterize the surface acidity of the as-formed α-Fe_2O_3. NH_3-TPD was carried out at 50–600°C in a microreactor. The temperature was measured using a K-type thermocouple. The molecules from the outlet of the microreactor were monitored using a quadrupole mass spectrometer (Hiden QIC-20, m/z = 15). Prior to desorption, the sample was saturated with NH_3 based on the m/z = 15 signal at a temperature of 50°C. Then, desorption was performed at a rate of 10 °C min^{-1} from 50 to 600°C.

RESULTS AND DISCUSSION

SCR Activity of the CNH Catalyst

The NO conversions over CNH catalysts with different reaction temperatures of 150, 200, 250, 300, 350, and 400°C are shown in Fig. 2(a). Similar to other iron oxides catalyst, the reaction temperature had a considerable effect on the NO conversion over the CNH catalysts. The NO conversion increased dramatically as the reaction temperature increased for all the selected catalysts. In addition, the NO conversion was significantly dependent on the preparation temperature of CNH. In particular, the increase in the reaction temperature favored the conversion of NO. Moreover, under the same reaction temperature, as the thermal treatment temperature decreased, the NO conversion increase, as shown in Fig. 2. The NO conversion reached 81.1–95.3% over CNH400 and CNH500, respectively, in contrast to 34–38.8% over CNH800 when the reaction temperature was 350–400°C. As the reaction temperature decreased to 300°C, the NO conversion over CNH400 and CNH500 remained at 80% but decreased to 52.98% and 21.98% over CNH700 and CNH800, respectively. These results indicated that the increase in the thermal treatment temperature went against the NO conversion. Therefore, the thermal treatment temperature is responsible for the remarkable difference in the SCR activity of the different CNH catalysts. The N_2 selectivity of all the catalysts gradually decreased above 300°C, and the N_2 selectivity of CNH400, CNH500, and CNH600 was higher than 80%, as shown in Fig. 1(b).

XRD

The XRD patterns of α-FeOOH and the thermally treated α-FeOOH are shown in Fig. 3. The reflections at 2θ = 21.3°, 33.3°, and 36.7° as well as 2θ = 24.2, 35.7°, and 39.3° were identified as goethite (α-FeOOH) and hematite (α-Fe_2O_3), respectively. The reflections of goethite disappeared and were replaced by those of hematite, indicating that the goethite was transformed into hematite when the thermal treatment temperature was more than 400°C. The decomposition of goethite, which occurs at more than 225°C, has been was previously reported (Rendon *et al.*, 1983; Serna and Iglesias, 1986; Liu *et al.*, 2013b). However, the intensity of the hematite reflections increased as the thermal treatment temperature increased, and well-defined hematite was obtained after thermal treatment at 800°C. The increasing temperatures contributed to increased crystallization of hematite. The existence of slightly remnant hydroxyl (-OH) hampered the crystallization of hematite until a high temperature was reached (i.e., 800°C in this study) (Schulze, 1984; Schulze and Schwertmann, 1987). In addition, the crystallization degree of hematite was inferred based on the increasing particle size of the (104) plane from 29 to 66 nm and the (110) plane from 36 to 56 nm as the temperature increased from 400°C to 800°C. The average particle size was calculated using the Scherrer equation.

Based on the XRD patterns and SCR reactivity, α-Fe_2O_3 was confirmed to be the active component for the SCR of NO, and the SCR reactivity was significantly affected by the pretreatment temperature. The SCR activity of α-Fe_2O_3 has been documented during the past three decades, and the corresponding mechanism has been extensively studied (Brandenberger *et al.*, 2010; Li *et al.*, 2011; Mou *et al.*, 2012b; Liu *et al.*, 2013a; Boroń *et al.*, 2015). In addition, both the L-H and E-R mechanisms have been extensively discussed for the SCR of NO reaction over different Fe-based oxide (iron oxides and Fe-based) catalysts (Chen *et al.*, 2010; Liu *et al.*, 2013a; Mejri *et al.*, 2016), where the E-R mechanism has been proposed as the main reaction route (Apostolescu *et al.*, 2006; Liu *et al.*, 2013a). Briefly,

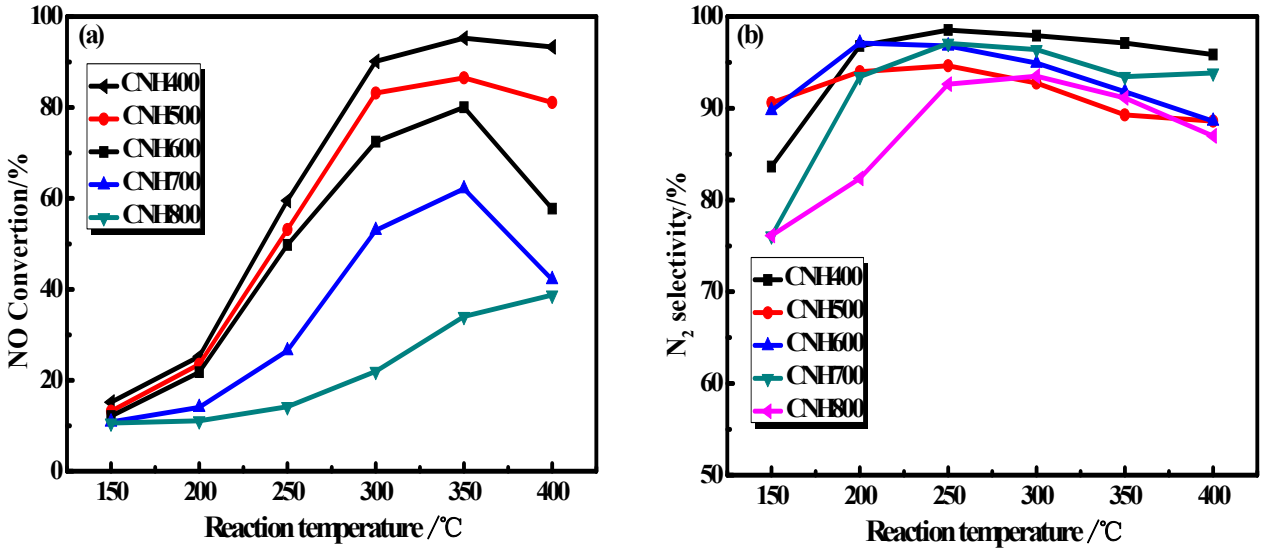

Fig. 2. SCR performances of different nanoporous α-Fe_2O_3 $_{catalysts}$: (a) NO conversion and (b) N_2 selectivity. (Reaction conditions: NO 500 ppm, NH_3 500 ppm, O_2 3 vol%, and balance of Ar, GHSV = 72,000 h^{-1}).

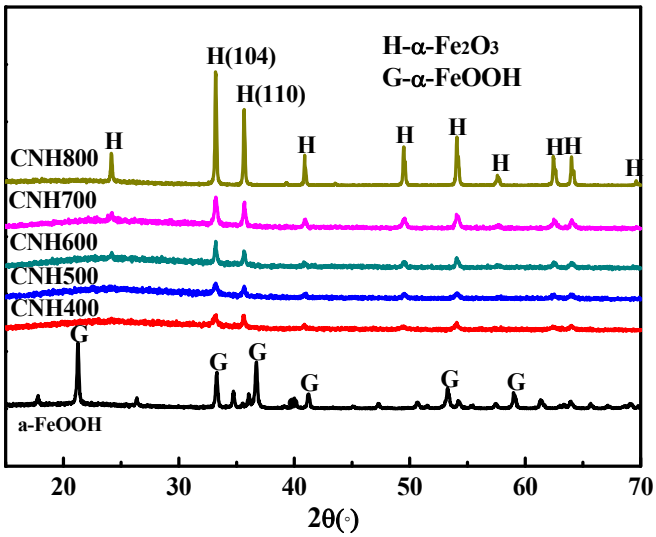

Fig. 3. XRD patterns of α-FeOOH and different nanoporous α-Fe_2O_3.

NH_3 is adsorbed on the surface of the iron oxides to form NH_4^+ and coordinated NH_3 followed by the reaction with gaseous NO to afford N_2 and H_2O. The amount of NH_4^+ and coordinated NH_3 were positively correlated to the amount of Bronsted and Lewis sites, respectively. In this study, α-Fe_2O_3, which was obtained by thermal treatment of α-FeOOH due to dihydroxylation, inevitably caused variation in the amount of surface hydroxyl groups as well as the pore structure at different temperatures. In detail, the peak area corresponding to the hydroxyl group (3000–3800 cm^{-1}) decreased from 2.90 to 0.45 as the temperature increased from 400°C to 800°C (results not shown here). The peak area was calculated by integration of the FT-IES results. The variation in both the surface hydroxyl and pore structure affected the surface acid-base properties. The increasing thermal treatment temperature favored the transformation of α-FeOOH to α-Fe_2O_3, resulting in a decrease in surface hydroxyl groups (i.e., surface acidic properties) and affects the SCR activity. Therefore, the decrease in surface hydroxyl groups is a possible reason for the decrease in the NO conversion.

TEM

To obtain representative images of nanoporous α-Fe_2O_3 as well as the effects of the temperature on the pore structure, HRTEM was employed to characterize CNH400, CNH500, CNH600, CNH700 and CNH800. The TEM images of α-FeOOH and thermally treated α-FeOOH (i.e., α-Fe_2O_3) at different temperatures are shown in Figs. 4(1) and 4(2). The spacing of the (104), (110) and (012) crystal planes was calculated and identified as the crystal plane of α-Fe_2O_3 using the XRD results. Therefore, α-FeOOH was transformed into α-Fe_2O_3, and the newly formed α-Fe_2O_3 retained the original shape of α-FeOOH, as shown in Fig. 4(1a). However, many pores can be observed in the images of CNH400,

CNH500 and CNH600 compared to the extremely few pores observed for CNH700 and CNH800. The pore was labeled with a red dashed line, as shown in Fig. 4(1d), and based on the TEM images, the pore distribution of CNH400, CNH500 and CNH600 is provided in Fig. 4(1b). A single crystal was selected to number and measure each sample. The pore size distributions of CNH400, CNH500 and CNH600 were centered at 0–3, 12–15 and 21–24 nm, respectively, indicating a shift to larger pore sizes as the temperature increased from 400°C to 600°C. In combination with the NO conversion shown in Fig. 2, the decrease in the pore as well as the increase in the pore size may decrease the surface area, resulting in a decrease in reactive sites as well as a decrease in the NO conversion.

These results indicate that the nanoporous α-Fe_2O_3 was prepared by thermal treatment of α-FeOOH, and the pore

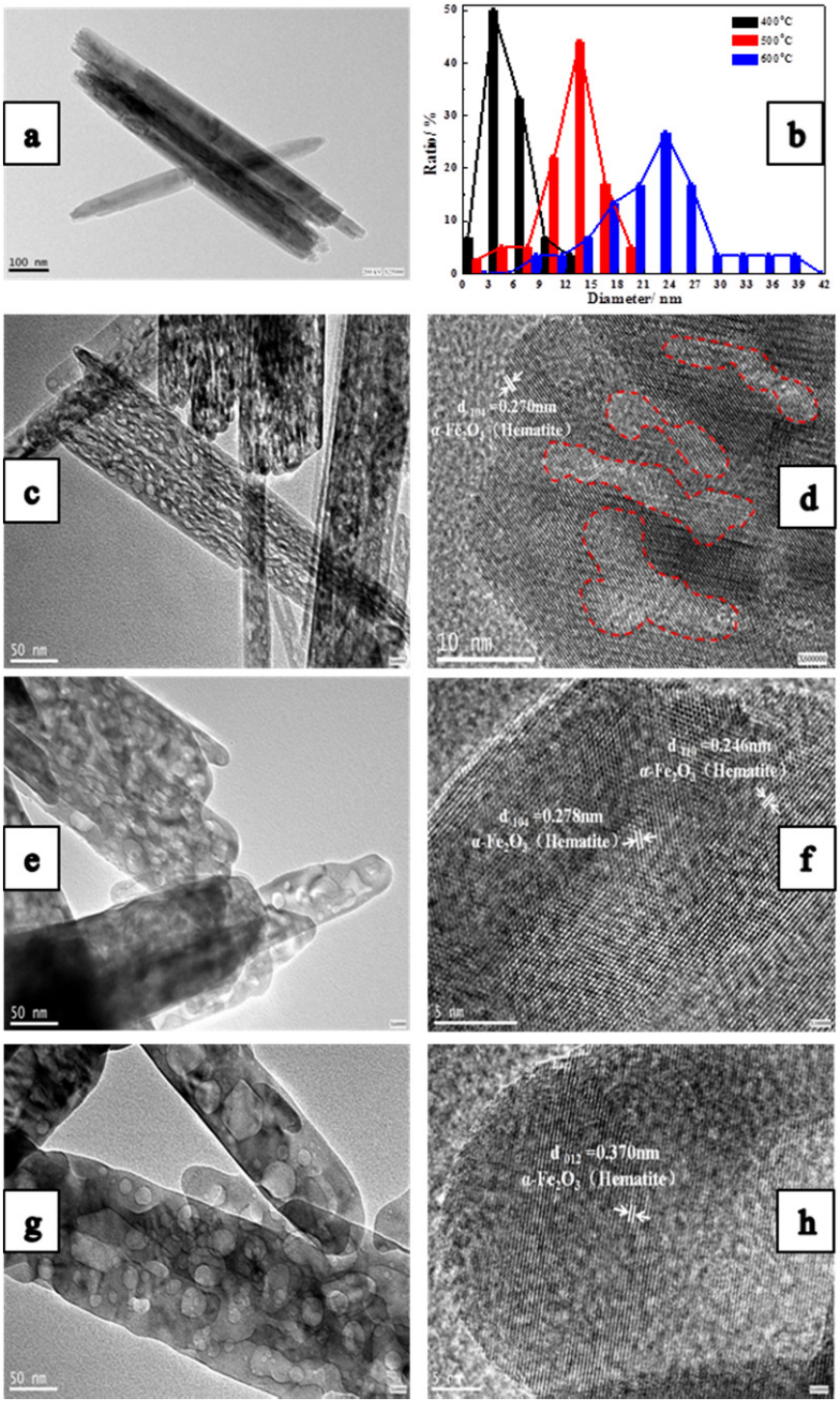

Fig. 4(1). HRTEM images of α-FeOOH (a), CNH400 (c, d), CNH500 (e, f) and CNH600 (g, h) and pore distribution of (b) CNH400, CNH500 and CNH600.

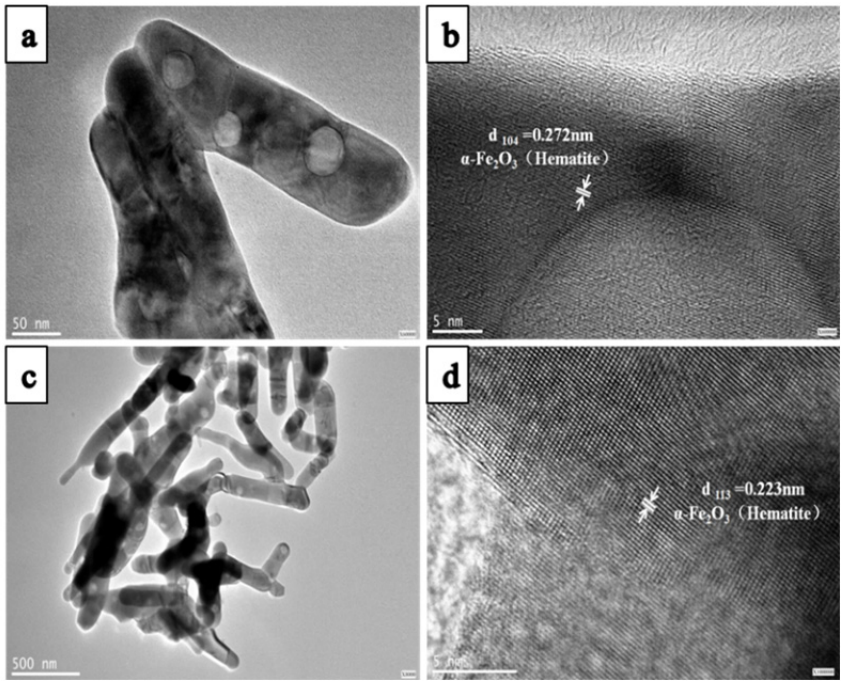

Fig. 4(2). HRTEM images of CNH700 (a, b) and CNH800 (c, d).

size can be controlled by adjusting the temperature. The increasing temperature decreased the number of pores and increased the pore size, which most likely decreased the NO conversion due to a decrease in the number of reactive sites.

Specific Surface Area and Pore Structure

To gain additional insight into the variation in the pore structure, the surface area, pore volume, average pore size and pore distribution were characterized using a pore size and surface area analyzer. The N_2 adsorption-desorption curves of five samples are shown in Fig. 5. All the isotherms were similar and close to type IV (i.e., porous property). However, at a high relative pressure, the hysteresis loop and amount of absorbed N_2 decreased as the thermal treatment temperature increased, indicating a decrease in the surface area. This result was in good agreement with the TEM images. In particular, the newly formed α-Fe_2O_3 embodied the microporous and mesoporous properties deduced from the results of the TEM images, N_2 adsorption-desorption curves and the pore distribution (Fig. 6), especially for the CNH400 catalyst. The textural properties were also represented by the specific surface area, pore volume, and average pore size data. As shown in Table 1, the surface area and pore volume of this series of catalysts decreased with increasing temperature, and the average pore size increased to 13.1 nm and then slightly decreased. The decrease in the former was due to a decrease in the number of pores and the increase in the pore size. In addition, the pore size and surface area of Fe_2O_3 prepared by thermal treatment at different temperatures were reproducible.

Catalysts with a large surface area are favorable to a catalytic reaction due to additional active sites. Therefore, excellent NO conversion was observed over the CNH400, CNH500, and CNH600 catalysts at 300°C. Moreover, at a reaction temperature of 250°C, the SCR activity of the catalysts increased in the following order: CNH800 < CNH700 < CNH600 < CNH500 < CNH400. However, the decrease in the surface area was not proportionate to the decrease in the NO conversion at a reaction temperature of 250°C. Therefore, the surface area had a considerable effect on the NO conversion, especially at low temperature, but was not the only factor.

XPS

To determine the state of oxygen on the surface of the catalysts, five types of catalysts were characterized using XPS, and the results are shown in Fig. 7. The O 1s band of the five samples exhibit one high peak with a large shoulder peak, and the intensity decreased with increasing thermal treatment temperature. To elaborate the O 1s band, Fig. 7 was deconvoluted under the same conditions. After deconvolution, the main peak at a lower binding energy (530–530.4 eV) and the shoulder peak at a lower binding energy (531.3–531.7 eV) were more obvious. To the best of our knowledge, the former peak was due to the lattice oxygen O^{2-} (denoted as O_β), and the latter peak corresponded to surface adsorbed oxygen (denoted as O_α) including defect oxide or surface hydroxyl groups (Liu *et al.*, 2011a, c; Liu *et al.*, 2013a). As shown in Fig. 7, a decrease in both types of peak areas as the thermal treatment temperature increased was observed, especially at 800°C. O_α are considered to be the active sites of the SCR of NO by providing acid sites to adsorb NH_3 molecules to form NH_4^+ and coordinated NH_3. In this study, thermal treatment led to dehydroxylation and restructuring of the iron oxide, resulting in the formation of defect oxygen. The increasing temperature also caused deep dehydroxylation and crystallization of α-Fe_2O_3, decreasing the surface area and

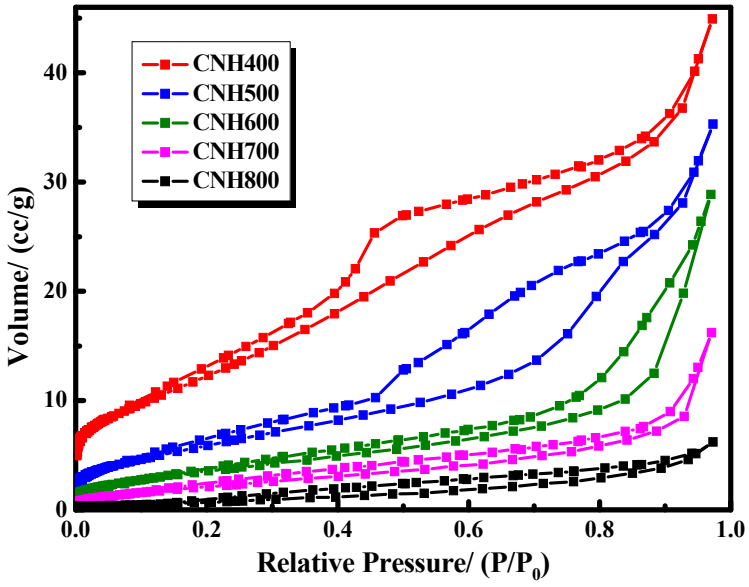

Fig. 5. N_2 adsorption-desorption curves of nanoporous α-Fe_2O_3.

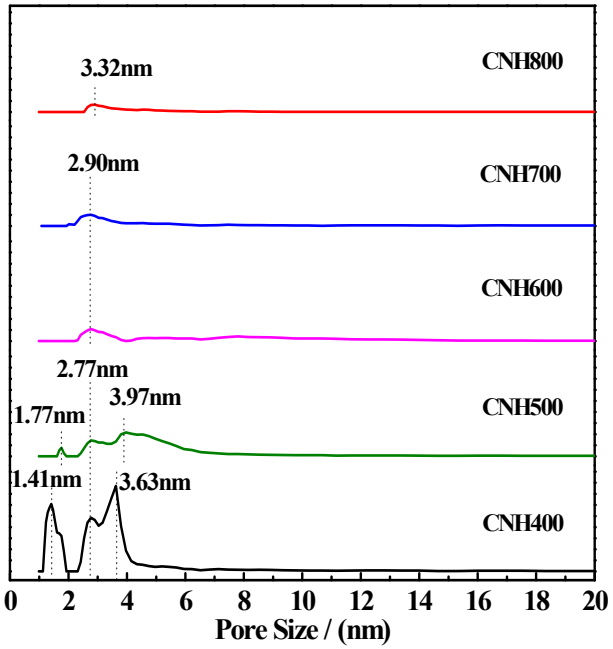

Fig. 6. Pore distribution of nanoporous α-Fe_2O_3.

the number of surface hydroxyl groups, increasing the crystallization degree and decreasing the O_α. Therefore, the decrease in O_α most likely leads to the decrease in the NO conversion.

In particular, the reaction between NH_4^+ due to the adsorption of NH_3 molecules on Brönsted acid sites and monodentate nitrate due to the oxidation of NO in the presence of O_2 has been proposed as the main reaction process at temperatures lower than 200°C (i.e., L-H mechanism) (Liu *et al.*, 2011c). However, the E-R mechanism replaces the L-H mechanism at temperatures higher than 200°C (Apostolescu *et al.*, 2006; Boroń *et al.*, 2015).

In this study, α-Fe_2O_3 exhibited excellent SCR activity at reaction temperatures higher than 200°C. Therefore, the E-R mechanism is regarded as the main reaction route for these catalysts. Therefore, the Brönsted acid sites do not play an important role in the catalytic SCR of NO by NH_3. In fact, CNH400 did not exhibit excellent SCR activity compared to the other catalysts even though CNH400 had the largest number of surface hydroxyl groups. Therefore, the existence of hydroxyl groups does not substantially improve the SCR activity. In addition, it is important to note that O_α substantially decreased as the thermal treatment temperature reached 800°C, and the NO conversion over CNH800 was remarkably low compared to that of other catalysts. The higher temperature favored an improved degree of crystallization of α-Fe_2O_3, decreasing the oxygen defect. Therefore, the decrease in oxygen defects directly decreased the SCR activity of α-Fe_2O_3. In addition, these results confirmed that the main route for the SCR of NO over iron oxide catalysts is consistent with the E-R mechanism rather than the L-H mechanism.

NH_3-TPD

The reaction mechanism of the SCR of NO could follow either the L-H mechanism or the E-R mechanism. Here, the activation of NH_3 is the key factor in the reaction process. To characterize the adsorption property of NH_3 on the surface of the newly formed α-Fe_2O_3 catalysts, NH_3-TPD was performed, and the curves are shown in Fig. 8. Moreover, the amount of adsorbed NH_3 was determined based on the NH_3-TPD curves. Three NH_3 desorption peak was clearly observed from 50°C to 500°C. As previously reported (Liu *et al.*, 2011c), the desorption of physisorbed NH_3 and Lewis acid sites with adsorbed NH_3 were observed at 54°C and 193°C, respectively. In addition, the desorption of NH_3 bound to strong Brönsted acid sites at a temperature of more than 350°C was confirmed (Ayari *et al.*, 2013; Mejri *et al.*, 2016). Therefore, the relatively higher desorption temperature of NH_3 in this study was due to the NH_3 bound to strong

Table 1. Surface area, pore volume, and average pore size of various nanoporous α-Fe_2O_3 catalysts.

Sample	BET/m^2 g^{-1}	Volume/cc g^{-1}	Pore Size/nm
CNH400	47.24	0.070	5.89
CNH500	22.67	0.055	9.63
CNH600	13.63	0.045	13.10
CNH700	8.50	0.025	11.81
CNH800	3.27	0.010	11.76

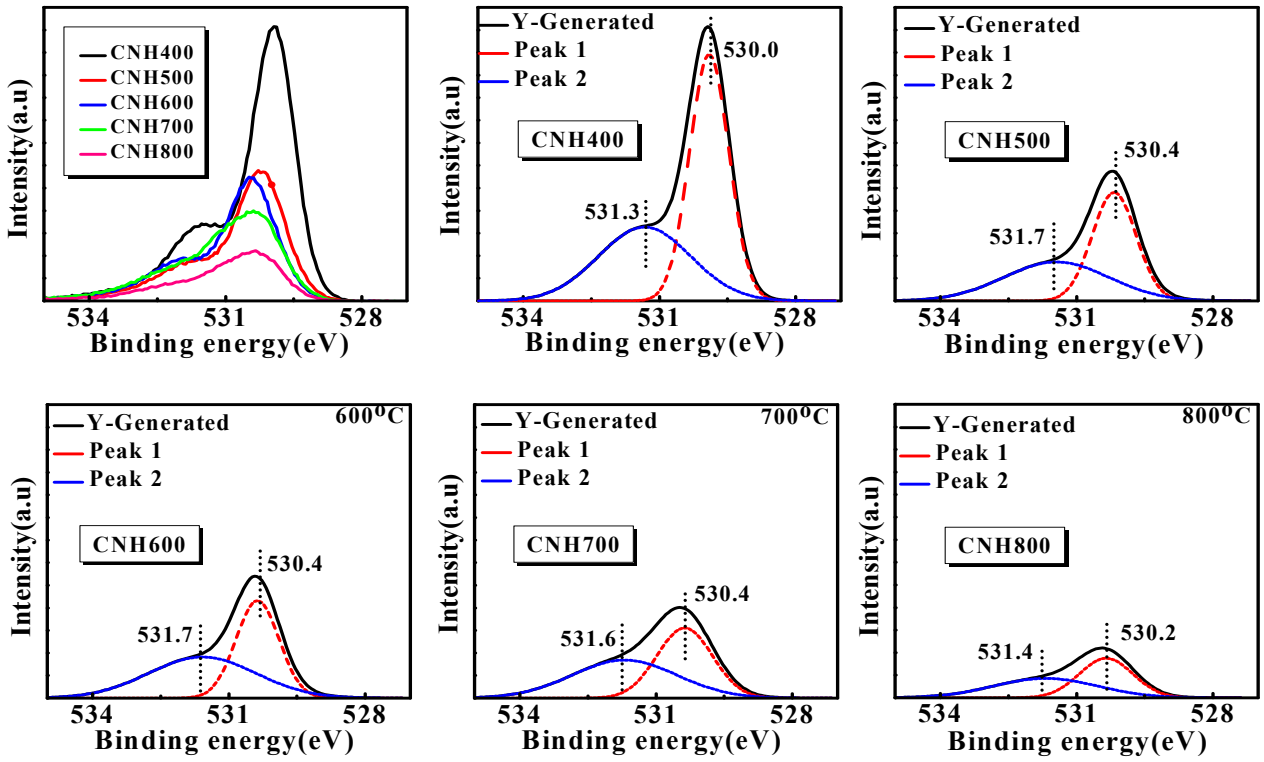

Fig. 7. XPS results of O 1 s of various nanoporous α-Fe_2O_3.

Brönsted acid sites derived from Fe-OH. The hydroxyl group resulted from the incomplete decomposition of α-FeOOH. The lower temperature contributed to physisorbed NH_3 and Lewis acid sites with adsorbed NH_3. The desorption temperature was higher than that previously mentioned (i.e., 54 and 193°C). The porous structure of α-Fe_2O_3 was also taken into consideration. The porous structure shown in the TEM images inhibited the desorption of physisorbed NH_3, which resulted in a high desorption temperature. The porous property also contributed to a large adsorption amount, and the amount decreased as the number of pores decrease. In particular, CNH400 exhibited the maximum NH_3 adsorption and desorption amounts. The calculated amount of adsorbed NH_3 increased in the following order: CNH800 (56.8 μmol g^{-1}) < CNH700 (71.2 μmol g^{-1}) < CNH600 (177.4 μmol g^{-1}) < CNH500 (296.9 μmol g^{-1}) < CNH400 (362.7 μmol g^{-1}).

CONCLUSIONS

Nanoporous hematite (α-Fe_2O_3) with different specific surface areas were prepared by thermal treatment of α-FeOOH. As the temperature increased from 400°C to 800°C, the surface area, average pore size and amount of adsorbed NH_3 varied from 47.24 m^2 g^{-1}, 5.89 nm and 56.8 μmol g^{-1}, respectively, to 3.27 m^2 g^{-1}, 11.76 nm and 362.7 μmol g^{-1}, respectively. The increasing thermal treatment temperature increased the average pore size and decreased the amount of adsorbed NH_3. In addition, the XPS results indicated that the increased temperature improved the crystallization of α-Fe_2O_3 and decreased the surface oxygen defects. With respect to the surface activity, the newly formed α-Fe_2O_3 exhibited excellent SCR activity, especially at reaction temperatures of more than 300°C. In combination with previous results, the E-R mechanism was proposed as the main route for the SCR of NO over α-Fe_2O_3 in this study. Goethite (α-FeOOH) naturally occurs on the surface of the Earth and can be easily obtained. This use of this type of natural mineral as the precursor for α-Fe_2O_3 will significantly decrease the catalyst cost and expand the application field of goethite. This study confirmed the SCR activity of the newly formed α-Fe_2O_3 that was derived from the decomposition of α-FeOOH and provided a theoretical principle for the application of natural goethite in the SCR of NO by NH_3.

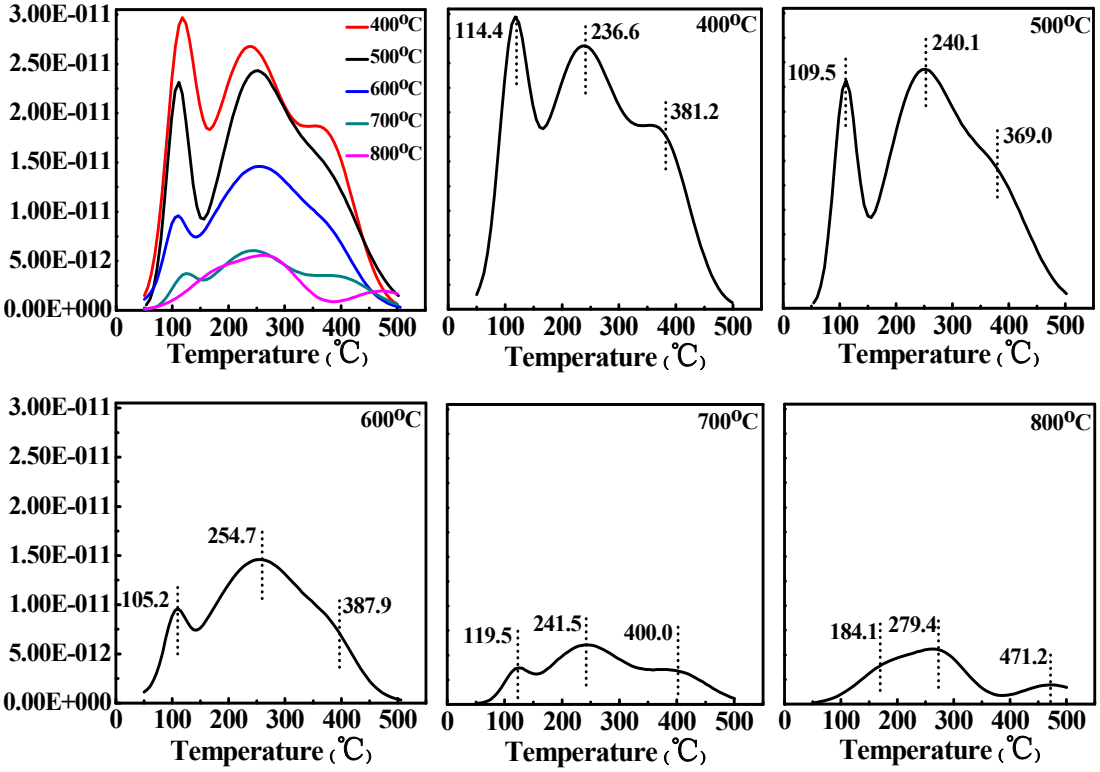

Fig. 8. NH_3-TPD curves of various nanoporous α-Fe_2O_3.

ACKNOWLEDGMENTS

This study was financially supported by the National Natural Science Foundation of China (No. 41402030, 41572029, 41372045), the China Postdoctoral Science Foundation funded project (No. 2014MM551794), the Fundamental Research Funds for the Central Universities (2014HGCH0007, JZ2017HGTB0196), and Anhui Provincial Natural Science Foundation (1708085MD87).

REFERENCES

Apostolescu, N., Geiger, B., Hizbullah, K., Jan, M.T., Kureti, S., Reichert, D., Schott, F. and Weisweiler, W. (2006). Selective catalytic reduction of nitrogen oxides by ammonia on iron oxide catalysts. *Appl. Catal. B* 62: 104–114.

Ayari, F., Mhamdi, M., Álvarez-Rodríguez, J., Guerrero Ruiz, A.R., Delahay, G. and Ghorbel, A. (2013). Cr-ZSM-5 catalysts for ethylene ammoxidation: Effects of precursor nature and Cr/Al molar ratio on the physicochemical and catalytic properties. *Microporous Mesoporous Mater.* 171: 166–178.

Balle, P., Geiger, B. and Kureti, S. (2009). Selective catalytic reduction of NO_x by NH_3 on Fe/HBEA zeolite catalysts in oxygen-rich exhaust. *Appl. Catal. B* 85: 109–119.

Boroń, P., Chmielarz, L., Gurgul, J., Łątka, K., Gil, B., Marszałek, B. and Dzwigaj, S. (2015). Influence of iron state and acidity of zeolites on the catalytic activity of FeHBEA, FeHZSM-5 and FeHMOR in SCR of NO with NH_3 and N_2O decomposition. *Microporous Mesoporous Mater.* 203: 73–85.

Brandenberger, S., Kröcher, O., Tissler, A. and Althoff, R. (2010). The determination of the activities of different iron species in Fe-ZSM-5 for SCR of NO by NH_3. *Appl. Catal. B* 95: 348–357.

Chen, J.P., Hausladen, M.C. and Yang, R.T. (1995). Delaminated Fe_2O_3-pillared clay: Its preparation, characterization, and activities for selective catalytic reduction of NO by NH_3. *J. Catal.* 151: 135–146.

Chen, L., Li, J. and Ge, M. (2010). Drift Study on cerium–tungsten/titiania catalyst for selective catalytic reduction of NO_x with NH_3. *Environ. Sci. Technol.* 44: 9590–9596.

Chen, T., Guan, B., Lin, H. and Zhu, L. (2014). In situ drifts study of the mechanism of low temperature selective catalytic reduction over manganese-iron oxides. *Chinese J. Catal.* 35: 294–301.

Chiu, C.H. (2015). Simultaneous control of elemental mercury/sulfur dioxide/nitrogen monoxide from coal-fired flue gases with metal oxide-impregnated activated carbon. *Aerosol Air Qual. Res.* 15: 2094–2103.

Duffy, B.L., Curry-Hyde, H.E., Cant, N.W. and Nelson, P.F. (1994). Effect of preparation procedure, oxygen concentration and water on the reduction of nitric oxide by ammonia over chromia selective catalytic reduction catalysts. *Appl. Catal. B* 5: 133–147.

Eigenmann, F., Maciejewski, M. and Baiker, A. (2006). Selective reduction of No by Nh_3 over manganese–cerium mixed oxides: Relation between adsorption, redox and catalytic behavior. *Appl. Catal. B* 62: 311–318.

Grossale, A., Nova, I., Tronconi, E., Chatterjee, D. and Weibel, M. (2009). NH_3-NO/NO_2 Scr for diesel exhausts

aftertreatment: reactivity, mechanism and kinetic modelling of commercial Fe- and Cu-promoted zeolite catalysts. *Top. Catal.* 52: 1837–1841.

Haibo, L., Tianhu, C., Chengsong, Q., Qiaoqin, X. and Frost, R.L. (2013). Confirmation of the assignment of vibrations of goethite: An ATR and IES Study of goethite structure. *Spectrochim. Acta, Part A* 116: 154–159.

Huang, H., Lan, Y., Shan, W., Qi, F., Xiong, S., Liao, Y., Fu, Y. and Yang, S. (2013). Effect of Sulfation on the selective catalytic reduction of NO with NH_3 over γ-Fe_2O_3. *Catal. Lett.* 144: 578–584.

Kang, M., Park, E.D., Kim, J.M. and Yie, J.E. (2007). Manganese oxide catalysts for NO_x reduction with NH_3 at low temperatures. *Appl. Catal. A* 327: 261–269.

Kapteijn, F., Singoredjo, L., Andreini, A. and Moulijn, J.A. (1994). Activity and selectivity of pure manganese oxides in the selective catalytic reduction of nitric oxide with ammonia. *Appl. Catal. B* 3: 173–189.

Kato, A., Matsuda, S., Nakajima, F., Imanari, M. and Watanabe, Y. (1981). Reduction of nitric oxide with ammonia on iron oxide-titanium oxide catalyst. *J. Phys. Chem.* 85:12: 1710–1713.

Khokhar, M.F., Yasmin, N., Fatima, N., Beirle, S. and Wagner, T. (2015). Detection of trends and seasonal variation in tropospheric nitrogen dioxide over Pakistan. *Aerosol Air Qual. Res.* 15: 2508–2524.

Kiros, F., Shakya, K.M., Rupakheti, M., Regmi, R.P., Maharjan, R., Byanju, R.M., Naja, M., Mahata, K., Kathayat, B. and Peltier, R.E. (2017). Variability of anthropogenic gases: Nitrogen oxides, sulfur dioxide, ozone and ammonia in Kathmandu Valley, Nepal. *Aerosol Air Qual. Res.* 16: 3088–3101.

Li, J., Chang, H., Ma, L., Hao, J. and Yang, R.T. (2011). Low-temperature selective catalytic reduction of NO_x with NH_3 over metal oxide and zeolite catalysts—A review. *Catal. Today* 175: 147–156.

Liu, C., Yang, S., Ma, L., Peng, Y., Hamidreza, A., Chang, H. and Li, J. (2013a). Comparison on the Performance of α-Fe_2O_3 and γ-Fe_2O_3 for Selective Catalytic Reduction of Nitrogen Oxides with Ammonia. *Catal. Lett.* 143: 697–704.

Liu, F. and He, H. (2010). Structure-activity relationship of iron titanate catalysts in the selective catalytic reduction of NO_x with NH_3. *J. Phys. Chem. C* 114: 16929–16936.

Liu, F., Asakura, K., He, H., Liu, Y., Shan, W., Shi, X. and Zhang, C. (2011a). Influence of calcination temperature on iron titanate catalyst for the selective catalytic reduction of NO_x with NH_3. *Catal. Today* 164: 520–527.

Liu, F., Asakura, K., He, H., Shan, W., Shi, X. and Zhang, C. (2011b). Influence of sulfation on iron titanate catalyst for the selective catalytic reduction of NO_x with NH_3. *Appl. Catal. B* 103: 369–377.

Liu, F., He, H., Zhang, C., Shan, W. and Shi, X. (2011c). Mechanism of the selective catalytic reduction of NO_x with NH_3 over environmental-friendly iron titanate catalyst. *Catal. Today* 175: 18–25.

Liu, H., Chen, T. and Frost, R.L. (2014). An overview of the role of goethite surfaces in the environment. *Chemosphere* 103: 1–11.

Liu, H., Chen, T., Zou, X., Qing, C. and Frost, R.L. (2013b). Effect of Al content on the structure of Al-substituted goethite: A micro-raman spectroscopic study. *J. Raman Spectrosc.* 44: 1609–1614.

Liu, H., Wei, L., Yue, R. and Chen, Y. (2010). Crox-Ceo_2 binary oxide as a superior catalyst for NO reduction with NH_3 at low temperature in presence of CO. *Catal. Commun.* 11: 829–833.

Ma, L., Li, J., Ke, R. and Fu, L. (2011). Catalytic performance, characterization, and mechanism study of $Fe_2(SO_4)_3/TiO_2$ catalyst for selective catalytic reduction of NO_x by ammonia. *J. Phys. Chem. C* 115: 7603–7612.

Ma, L., Chang, H., Yang, S., Chen, L., Fu, L. and Li, J. (2012). Relations between iron sites and performance of Fe/HBEA catalysts prepared by two different methods for NH_3-SCR. *Chem. Eng. J.* 209: 652–660.

Mejri, I., Ayari, F., Mhamdi, M., Delahay, G., Ksibi, Z. and Ghorbel, A. (2016). SCR of NO by NH_3 catalyzed by Mo- and V-exchanged zeolite: Effect of Mo precursor salt. *Microporous Mesoporous Mater.* 220: 239–246.

Mou, X., Zhang, B., Li, Y., Yao, L., Wei, X., Su, D.S. and Shen, W. (2012a). Rod-shaped Fe_2O_3 as an efficient catalyst for the selective reduction of nitrogen oxide by ammonia. *Angew. Chem. Int. Ed.* 51: 2989–2993.

Ochońska, J., McClymont, D., Jodłowski, P.J., Knapik, A., Gil, B., Makowski, W., Łasocha, W., Kołodziej, A., Kolaczkowski, S.T. and Łojewska, J. (2012). Copper exchanged ultrastable zeolite Y-A catalyst for NH_3-SCR of NO_x from stationary biogas engines. *Catal. Today* 191: 6–11.

Perezramirez, J. (2004). Reduction of N_2O with CO over FeMFI zeolites: Influence of the preparation method on the iron species and catalytic behavior. *J. Catal.* 223: 13–27.

Rendon, J.L., Cornejo, J., de Arambarri, P. and Serna, C.J. (1983). Pore structure of thermally treated goethite (A-Feooh). *J. Colloid Interface Sci.* 92: 508–516.

Sahu, S.K. (2015). High resolution emission inventory of NO_x and CO for mega city Delhi, India. *Aerosol Air Qual. Res.* 15: 1137–1144.

Schneider, H., Maciejewski, M., Kohler, K., Wokaun, A. and Baiker, A. (1995). Chromia Supported on titania: Vi. Properties of different chromium oxide phases in the catalytic reduction of NO by NH_3 studied by in situ diffuse reflectance ftir spectroscopy. *J. Catal.* 157: 312–320.

Schulze, D.G. (1984). The influence of aluminum on iron oxides. VIII. Unit-cell dimensions of Al substituted goethites and estimation of Al from them. *Clays Clay Miner.* 32: 36–44.

Schulze, D.G. and Schwertmann, U. (1987). The influence of aluminium on iron oxides: XIII. Properties of goethites synthesised in 0-3 M KoOH at 25°C. *Clay Miner.* 22: 83–92.

Schuricht, F. and Reschetilowski, W. (2012). Simultaneous selective catalytic reduction (SCR) of NO_x and N_2O over Ag/ZSM-5-catalytic studies and mechanistic implications. *Microporous Mesoporous Mater.* 164: 135–144.

Serna, C.J. and Iglesias, J.E. (1986). Nature of

protohaematite and hydrohaematite. *J. Mater. Sci. Lett.* 5: 901–902.

Xu, W., Yu, Y., Zhang, C. and He, H. (2008). Selective catalytic reduction of NO by NH_3 over a Ce/TiO_2 catalyst. *Catal. Commun.* 9: 1453–1457.

Yang, R.T., Chen, J.P., Kikkinides, E.S., Cheng, L.S. and Cichanowicz, J.E. (1992). Pillared Clays as superior catalysts for selective catalytic reduction of NO with NH_3. *Ind. Eng. Chem. Res.* 31: 1440–1445.

Yang, S., Wang, C., Chen, J., Peng, Y., Ma, L., Chang, H., Chen, L., Liu, C., Xu, J., Li, J. and Yan, N. (2012). A novel magnetic Fe–Ti–V spinel catalyst for the selective catalytic reduction of NO with NH_3 in a broad temperature range. *Catal. Sci. Technol.* 2: 915.

Yang, S., Liu, C., Chang, H., Ma, L., Qu, Z., Yan, N., Wang, C. and Li, J. (2013). Improvement of the activity of γ-Fe_2o_3 for the selective catalytic reduction of NO with NH_3 at high temperatures: No reduction versus NH_3 oxidization. *Ind. Eng. Chem. Res.* 52: 5601–5610.

Yang, S., Qi, F., Xiong, S., Dang, H., Liao, Y., Wong, P.K. and Li, J. (2016). Mnox supported on Fe-Ti spinel: A novel mn based low temperature SCR catalyst with a High N_2 selectivity. *Appl. Catal. B* 181: 570–580.

Yoshida, M. (2004). Structure sensitivity of ion-exchanged Fe-Mfi in the catalytic reduction of nitrous oxide by methane under an excess oxygen atmosphere. *J. Catal.* 223: 454–464.

Yu, C. (2015). In situ drifts study of the low temperature selective catalytic reduction of NO with NH_3 over mnox supported on multi-walled carbon nanotubes catalysts. *Aerosol Air Qual. Res.* 2015: 1017–1027.

Yu, X., Cao, F., Zhu, X., Zhu, X., Gao, X., Luo, Z. and Cen, K. (2017). Selective catalytic reduction of NO over Cu–Mn/OMC catalysts: Effect of preparation method. *Aerosol Air Qual. Res.* 17: 302–313.

Zahaf, R. (2015). Pt catalyst over SiO_2 and Al_2O_3 supports synthesized by aerosol method for HC-SCR denox application. *Aerosol Air Qual. Res.* 15: 2409–2421.

Zhu, Z., Liu, Z., Liu, S., Niu, H., Hu, T., Liu, T. and Xie, Y. (2000). NO reduction with NH_3 over an activated carbon-supported copper oxide catalysts at low temperatures. *Appl. Catal. B* 26: 25–35.

Received for review, May 7, 2016
Revised, June 19, 2017
Accepted, June 19, 2017